Acta Mechanica Sinica (2020) 36(2):397–411
https://doi.org/10.1007/s10409-020-00931-w

REVIEW PAPER

Theoretical models for irradiation hardening and embrittlement in nuclear structural materials: a review and perspective

Xiazi Xiao[1] · Dmitry Terentyev[2] · Haijian Chu[3] · Huiling Duan[4,5]

Received: 6 October 2019 / Accepted: 23 December 2019 / Published online: 27 February 2020

Abstract

The study of irradiation hardening and embrittlement is critically important for the development of next-generation structural materials tolerant to neutron irradiation, and could dramatically affect the approach to the design of components for advanced nuclear reactors. In addition, a growing interest is observed in the field of research and development of irradiation-resistant materials. This review aims to provide an overview of the theoretical development related to irradiation hardening and embrittlement at moderate irradiation conditions achieved in recent years, which can help extend our fundamental knowledge on nuclear structural materials. After a general introduction to the irradiation effects on metallic materials, recent research progress covering theoretical modelling is summarized for different types of structural materials. The fundamental mechanisms are elucidated within a wide range of temporal and spatial scales. This review closes with the current understanding of irradiation hardening and embrittlement, and puts some perspectives deserving further study.

Keywords Irradiation hardening · Irradiation embrittlement · Theoretical models · Fundamental mechanisms

1 Introduction

1.1 Motivation

With increasing energy demand for our daily life, growing economical development, and limited reserve of fossil fuel on earth, it has become urgent to develop novel non-fossil energy sources that can, on the one hand, effectively replace the contribution of conventional fossil energy, and on the other hand, be environmentally friendly and safe for the sustainable development of our next generations [1]. Among several alternative non-fossil energy sources (e.g. tidal energy, solar energy and wind energy), the nuclear energy is considered to be the promising one for our future development.

Generally speaking, the production route of nuclear energy can be divided into the fission and fusion type. Fission energy has already been serving human beings for more than half-century. Whereas, the shortcomings of fission energy, e.g. the low utilization of fission fuels and certain risks for the safe operation of nuclear reactors, push nuclear technology towards fusion energy. If it succeeds, it is likely to reduce the radioactivity and increase the safety in operation, as well as to solve the energy problem once and for all. Because of these promising advantages, the development of fusion energy has drawn an increasing attention over the last

Electronic supplementary material The online version of this article (https://doi.org/10.1007/s10409-020-00931-w) contains supplementary material, which is available to authorized users.

✉ Huiling Duan
hlduan@pku.edu.cn

Xiazi Xiao
xxz2017@csu.edu.cn

Dmitry Terentyev
dmitry.terentyev@sckcen.be

Haijian Chu
hjchu@shu.edu.cn

1 Department of Mechanics, School of Civil Engineering, Central South University, Changsha 410075, China

2 Structural Materials Group, Institute of Nuclear Materials Science, SCK-CEN, 2400 Mol, Belgium

3 Shanghai Key Laboratory of Mechanics in Energy Engineering, Shanghai Institute of Applied Mathematics and Mechanics, School of Mechanics and Engineering Science, Shanghai University, Shanghai 200444, China

4 State Key Laboratory for Turbulence and Complex System Department of Mechanics and Engineering Science, College of Engineering, Peking University, Beijing 100871, China

5 CAPT, HEDPS and IFSA Collaborative, Innovation Center of MoE, BIC-ESAT, Peking University, Beijing 100871, China

decades. The famous international nuclear fusion research projects, International Thermonuclear Experimental Reactor (ITER), started in 2006, aims to help the design and implementation of a full-scale electricity-producing demonstration fusion power station (DEMO), targeted for construction by 2050 [2].

To ensure the sustainable operation of nuclear reaction in the reactors, there exist a number of critical issues that need to be addressed. Thereinto, the research and development (R&D) of irradiation-resistant materials that can ensure the structural integrity and guarantee the safe exploition of components in nuclear reactors is extremely important. Under fusion operation conditions, structural materials would suffer from the impact of high flux neutrons and ions. The induced irradiation damage level is much higher than what is achieved in the fission reactors. So far, there is no such qualified material that can withstand the required irradiation conditions and, at the meantime, satisfy the requirements from the aspect of design [2].

1.2 Irradiation effect on nuclear structural materials

Depending on the periodic arrangement of material atoms, nuclear structural materials can be categorized into crystalline and non-crystalline ones. The latter type including amorphous solids is not discussed in this work. For metallic materials with crystalline structures, atoms are located in their Bravais lattices with well-defined periodic configurations. According to the type of Bravais lattices [3], metallic materials can be mainly divided into three categories: face centered cubic (FCC), body centered cubic (BCC), and hexagonal close packed (HCP) structures. Under a long-term exposure in the irradiation field, the mechanical properties of structural materials could be dramatically degraded when compared to the unirradiated state, which is termed as the irradiation damage effects on mechanical properties (see Fig. 1 for instance). There are four major types of the irradiation-induced degradation, which are determined by the irradiation dose and temperature [3]. At low irradiation temperature ($< T_m/6$, where T_m is the melting point), irradiation hardening and subsequent embrittlement are of primary concern [4]. With the increase of the irradiation temperature (up to $T_m/3$), irradiation-assisted creep becomes a major concern that the creep deformation is related to the irradiation dose, applied stress and gas bubbles [5]. Irradiation swelling originating from the formation and growth of voids can induce unacceptable dimensional changes at high irradiation dose in the intermediate temperature range (peak swelling occurs at the irradiation temperature of $T_m/4$) [6]. At high irradiation dose and high temperature, the accumulation and diffusion of transmutation gaseous elements such as helium (He) and hydrogen (H) can lead to the formation of gas bubbles in the grain boundaries that weakens the interface strength and promotes the intergranular fracture, which is called the hight temperature He embrittlement [7].

The occurrence of irradiation damage actually stems from the impact of energetic particles that generates lattice damage [8–10]. An impinging particle (e.g. swift ions, fast neutrons and MeV-range electrons) creates the primary knock-on atom (PKA) as a result of the scattering on the atoms that form the material's lattice. PKA generates a displacement cascade, which results in the formation of point defects and defect clusters [11]. High energy neutrons can also result in the nuclear transmutation leading to the generation of He by the (n, α) reaction. These defects, all together, are named as the primary irradiation-induced defects. Further diffusion and coalescence of these primary irradiation-induced defects lead to the establishment of nano-metric defects, which can suppress the plastic deformation and therefore impact the mechanical properties of irradiated materials [12]. The parameter defining irradiation dose is called fluence, and it represents a number of high energy particles per square meter. The concept of displacement per atom (DPA) is introduced to define the equivalent irradiation damage dose in materials with different lattice properties, which are exposed to different types of irradiation particles. One DPA means a displacement of each atom from its equilibrium lattice site, statistically.

The dominant irradiation-induced defects can be subdivided into four groups: (1) point defects, such as interstitials and vacancies [8,9], and new chemical elements generated as a result of transmutation; (2) one-dimensional defects like dislocations formed in neutron-irradiated copper [13]; (3) two-dimensional or planar defects such as dislocation loops (DLs) [14] as illustrated in Fig. 2a, which are observed in BCC iron after irradiation up to 0.3 DPA at 773 K; (4) three-dimensional defects such as solute rich clusters (as shown in Fig. 2b) [15], stacking fault tetrahedra (SFTs as shown in Fig. 2c) [16], and voids (Fig. 2d) [17] as noticed in SUS316L austenitic stainless steels. These irradiation-induced defects, formed at nano-scale, eventually influence the macroscopic mechanical properties of nuclear structural materials.

The study of how irradiation defects affect the macroscopic mechanical properties of metallic materials is a typical multi-scale problem [11,15,18–32]. Irradiation-induced defects formed at nano-scale affect the evolution of microstructures (e.g. dislocation-type defects, precipitation and interface structures) at meso-scale, which results in the alternated mechanical properties at macro-scale. Therefore, the combined investigation by numerical simulations, experimental observations and theoretical modelling at different scales plays a dominant role for the comprehension of irradiation effects, as presented in Fig. 3. Moreover, this multi-scale study method could further help the R&D of structural mate-

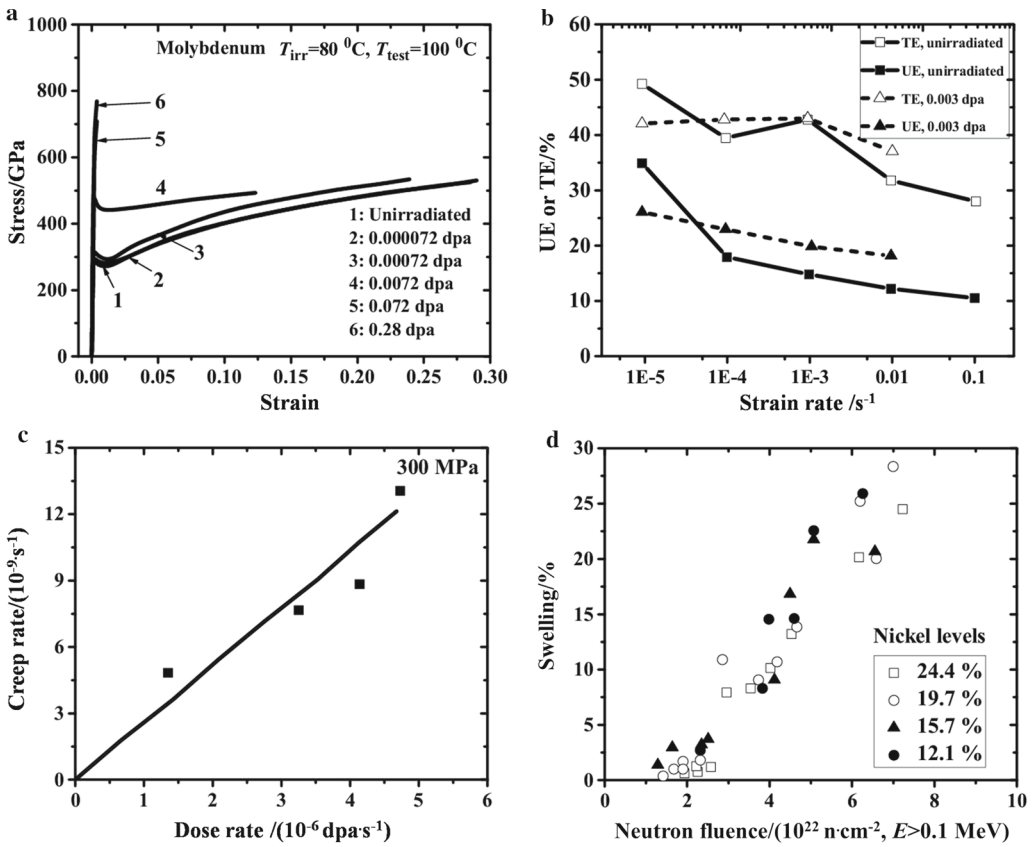

Fig. 1 Irradiation effect on the mechanical behavior of nuclear structural materials. **a** Stress–strain relationships of molybdenum under different irradiation doses when the irradiation temperature is 353 K. (Reprinted with permission from Ref. [4]. Copyright 2008 by Elsevier). **b** Irradiation effect on the uniform elongation (UE) and total elongation (TE) for unirradiated and irradiated molybdenum at different strain rates. (Reprinted with permission from Ref. [4]. Copyright 2008 by Elsevier). **c** Influence of dose rate on the irradiation creep of 20% cold-worked 316 stainless steel at 573 K. (Reprinted with permission from Ref. [6]. Copyright 1997 by Elsevier). **d** Effect of neutron fluence on the swelling of Fe-15Cr-Ni alloys for different nickel levels and temperatures in EBR-II. (Reprinted with permission from Ref. [5]. Copyright 2000 by Elsevier)

rials [33,34] that can be utilized in the future fusion and fission reactors.

1.3 Architecture

In this review, we focus on the irradiation hardening and embrittlement phenomena observed at intermediate temperature range ($T_m/6$–$T_m/3$) and up to moderate doses (several DPA), thus excluding the influence of transmutation-originated gases. The attention is primarily paid to the materials that have structural function in nuclear reactor components. The paper is organized as follows: in Sects. 2 and 3, we summarize the recent developments of theoretical models for the irradiation hardening and embrittlement. The former covers the conventional irradiation hardening model and crystal plasticity theory based irradiation hardening model, and the latter contains the theories proposed for the irradiation embrittlement. Summary and outlook messages are collected in Sect. 4.

2 Theoretical model for irradiation hardening

Due to the existence of irradiation-induced defects, the yield stress or hardness of irradiated materials is generally higher than that of their unirradiated counterparts. To theoretically explain this phenomenon, unremitting efforts have been made in the last decades [33–38]. Here, we subdivide the irradiation hardening model into two types, i.e. the conventional irradiation hardening model and crystal plasticity based irradiation hardening model.

2.1 Conventional irradiation hardening model

Based on the modified form of the Orowan theory [39] for the bowing of dislocation segments around impenetrable obstacles, the dispersed barrier hardening (DBH) model is proposed with the assumption that the increase of the critical resolved shear stress (CRSS) originates from the thermally and stress activated cutting of obstacles (arranged in regular array) by dislocations [40], i.e.

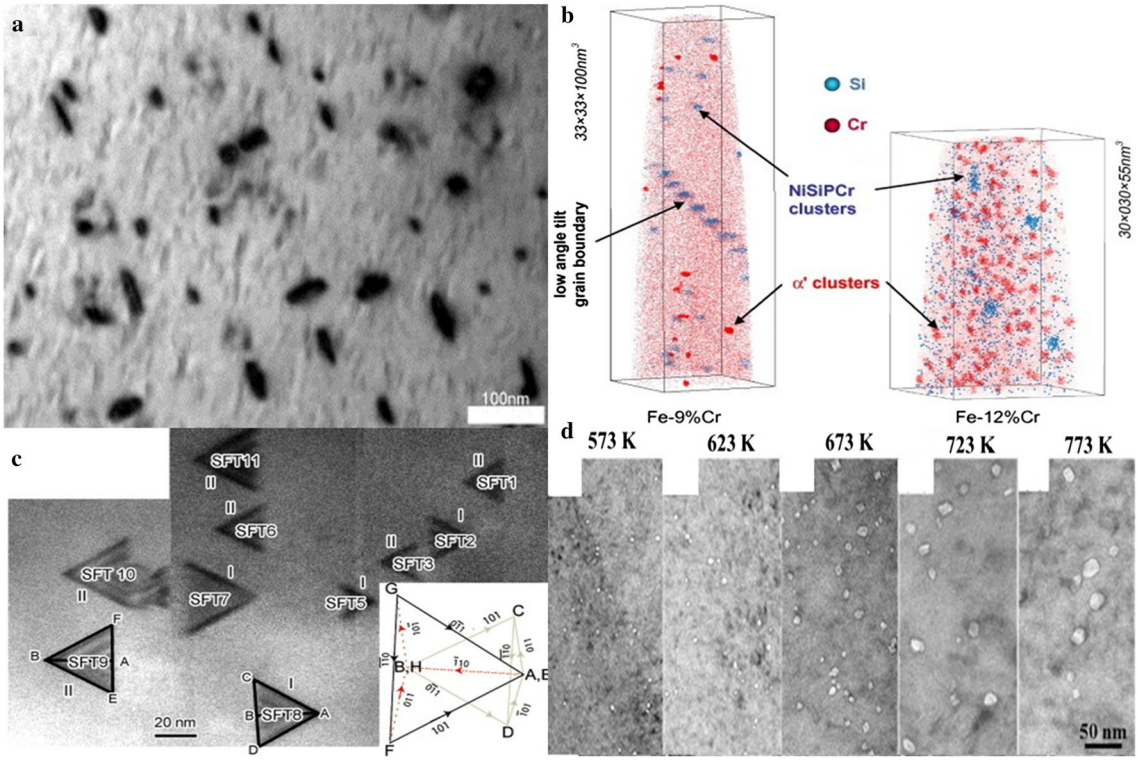

Fig. 2 Irradiation-induced defects formed under different irradiation conditions in various kinds of metallic materials. **a** DLs observed in iron after irradiation up to 0.3 DPA/180 appm He at 773 K. (Reprinted with permission from Ref. [14]. Copyright 2011 by Elsevier). **b** Cr rich clusters detected in Fe–Cr alloys after neutron irradiation at 573 K up to 0.6 DPA. (Reprinted with permission from Ref. [15]. Copyright 2012 by Elsevier). **c** SFTs observed in gold. (Reprinted with permission from Ref. [16]. Copyright 2013 by Elsevier). **d** Voids detected in SUS316L austenitic stainless steels under electron irradiation. (Reprinted with permission from Ref. [17]. Copyright 2017 by Elsevier)

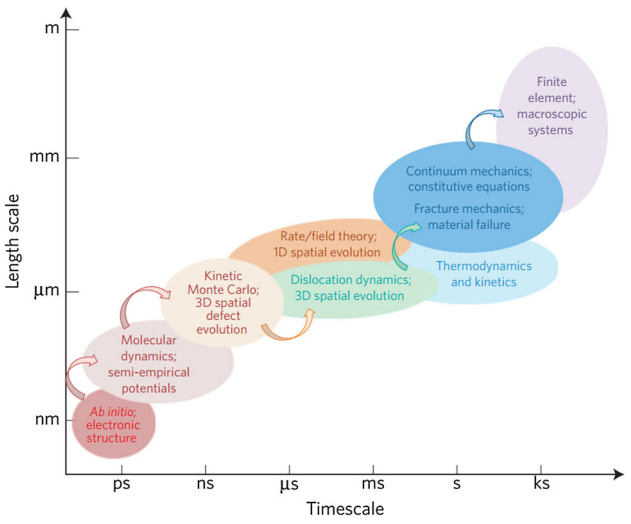

Fig. 3 Typical multi-scale computational methods for the comprehension of irradiation effect on material properties . (Reprinted with permission from Ref. [20]. Copyright 2016 by Macmillan Publishers)

$$\tau_{\mathrm{CRSS}} = h_{\mathrm{d}}\mu b/l = h_{\mathrm{d}}\mu b\sqrt{N_{\mathrm{def}}d_{\mathrm{def}}}, \tag{1}$$

where h_{d}, μ, b, N_{def} and d_{def} are, respectively, the interaction strength coefficient, shear modulus, magnitude of the Burgers vector, number density of the defect and defect size. $l = (N_{\mathrm{def}}d_{\mathrm{def}})^{-1/2}$ is the average spacing between obstacles (for the randomly distributed defects). According to Eq. (1), one can see that: (1) the DBH model is based on the assumption that a sufficient number of mobile dislocations is available. In the absence of grown-in dislocations, the DBH model does not hold; (2) the DBH model is proposed to correlate the yield stress with the density of irradiation-induced microstrutures, but contains no information on the work hardening behavior of irradiated materials; (3) small clusters are not appropriate obstacles to the sliding dislocations as required by the Orowan mechanisms [40]. For the sake of weak obstacle, the Friedel–Kroupa–Hirsch (FKH) model [41,42] is proposed to address the less extensive shearing of dislocations (i.e. the passage over weak obstacles), and is expressed as

$$\tau_{\mathrm{CRSS}} = \frac{1}{8}h_{\mathrm{d}}\mu b N_{\mathrm{def}}^{\frac{2}{3}}d_{\mathrm{def}}. \tag{2}$$

When applying the DBH model to either voids or loops made of self-interstitial atoms (SIAs), it is found that the

hardening behavior can hardly be reproduced without changing the defect strength coefficient as a function of the defect size [35]. Therefore, the Bacon–Kocks–Scattergood (BKS) model [43] is proposed for a fixed defect strength coefficient, i.e.

$$\tau_{\mathrm{CRSS}} = h_{\mathrm{d}} \frac{\mu b}{2\pi l} \left[\ln\left(\frac{l}{b}\right)\right]^{-\frac{1}{2}} \left[\ln\left(\frac{d'}{b}\right) + 0.7\right]^{\frac{3}{2}}, \tag{3}$$

with $d' = d_{\mathrm{def}} l/(d_{\mathrm{def}} + l)$. The approach proposed by Bacon et al. [43] in 1973 accounts for the self-interaction of dislocation arms, and therefore provides a more reliable solution in the case of strong obstacles when compared with the Orowan formula.

Unlike the Orowan-type hardening model, Singh et al. [40] suggested that the irradiation hardening should be treated by the cascade induced source hardening mechanism (CISH), i.e. the irradiation-induced small and glissile clusters made up of SIAs are mobile before they are trapped in the vicinity of dislocations. With the decoration of these small defects, the dislocations can hardly act as the Frank–Read sources until they are unpinned. The expression of the CISH model reads as:

$$\tau_{\mathrm{CISH}} = 0.1\mu(b/l)(d_{\mathrm{def}}/y)^2, \tag{4}$$

where τ_{CISH} is the applied shear stress, and y is the distance between the decorated defects and glissile dislocations. Based on Eq. (4), it can be seen that the stress to unlock the pinned dislocations not only increases with the decrease of the DL spacing, but also depends on the ratio of the defect size and distance between DLs and glissile dislocations. Moreover, the mechanisms of both discontinuous yielding and the formation of defect free channels can be qualitatively explained within the framework of the CISH [40].

It should be noted that the above mentioned hardening models (DBH, FKH, BKS, and CISH) are only be applicable under the condition of neutron irradiation, where the irradiation-induced defects are uniformly distributed throughout the whole sample. Whereas, for the case of ion irradiation, these hardening models should be modified due to the limited depth of the irradiation region and non-uniform distribution of defects in the irradiated layer [44–48]. As a modification of the DBH model, an average defect density based hardening model has been proposed for ion-irradiated materials [49–51], i.e.

$$\tau_{\mathrm{CRSS}} = h_{\mathrm{d}} \mu b \sqrt{\bar{N}_{\mathrm{def}} d_{\mathrm{def}}}, \tag{5}$$

where $\bar{N}_{\mathrm{def}}$ is the average defect density during the indentation experiments, which depends on the distribution of the defect density in the irradiated layer, shape and size of the plasticity affected region, and indentation depth. Based on experimental observations, the non-uniformly distributed irradiation defects can be assumed to follow as

$$N_{\mathrm{def}}(x) = \begin{cases} \left(\frac{x}{L_{\mathrm{d}}}\right)^n N^0_{\mathrm{def}}, & \text{for} \quad x \le L_{\mathrm{d}}, \\ 0, & \text{for} \quad x > L_{\mathrm{d}}, \end{cases} \tag{6}$$

where n and N^0_{def}, respectively, indicate the distribution profile of irradiation defects and peak value of the defect density. L_{d} is the maximum depth of the irradiated zone. When the formed plasticity region is within the irradiated region, $\bar{N}_{\mathrm{def}}$ can be derived as

$$\bar{N}_{\mathrm{def}}(h) = \frac{3N^0_{\mathrm{def}}(M_{\mathrm{r}}h)^n}{(n+1)(n+3)L^n_{\mathrm{d}}}, \quad \text{for} \quad h \le h^{\mathrm{sep}}_{\mathrm{c}}. \tag{7}$$

where h and $h^{\mathrm{sep}}_{\mathrm{c}}$ are, respectively, the indentation depth and critical indentation depth at which the plasticity affected region reaches L_{d}. M_{r} is the ratio coefficient between the radius of the plasticity affected region and indentation depth. With $h > h^{\mathrm{sep}}_{\mathrm{c}}$, $\bar{N}_{\mathrm{def}}$ can be deduced as

$$\bar{N}_{\mathrm{def}}(h) = \frac{3N^0_{\mathrm{def}}L_{\mathrm{d}}}{2(M_{\mathrm{r}}h)^3}\left[\frac{(M_{\mathrm{r}}h)^2}{n+1} - \frac{L^2_{\mathrm{d}}}{n+3}\right], \quad \text{for} \quad h > h^{\mathrm{sep}}_{\mathrm{c}}. \tag{8}$$

To connect the CRSS with the yield stress of irradiated polycrystals, an empirical formula has been widely adopted [52], i.e.

$$\sigma_{\mathrm{YS}} = M\tau_{\mathrm{CRSS}}, \tag{9}$$

where M is the Taylor factor characterizing the heterogeneous properties of individual grains with different grain orientations. The application of this modified DBH model (Eq. (5)) has been performed [49–51] to evaluate the increase of hardness as a function of the indentation depth for ion-irradiated Ni-17Mo-7Cr alloys [53], China-A508 steels [54], 16MND5 stees [55] and Fe-9Cr alloy [56], and the reasonable agreement between the theoretical results and experimental data indicates that both the inhomogeneously distributed defects and unirradiated substrate should be considered when analyzing the irradiation hardening behavior of ion-irradiated materials.

When there exist different types of irradiation-induced defects, the assumption of linear and square superposition laws has been widely applied to characterize the hardening contribution with different obstacle strengths [38,50,51]. For neutron-irradiated materials, the linear superposition law seems to work well within the framework of crystal plasticity theory [57]. When the difference of the obstacle strength

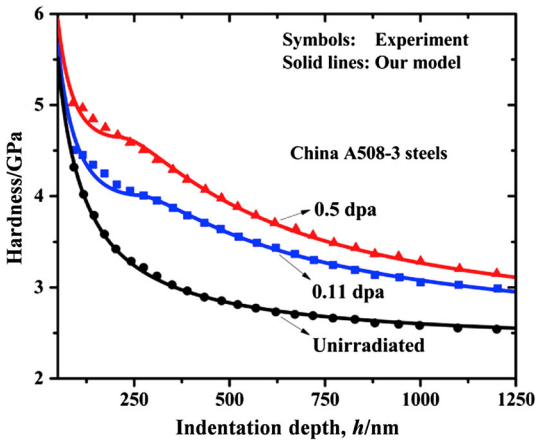

Fig. 4 Hardness-depth relationships compared between experimental data and theoretical results for China-A508 steels [54] . (Reprinted with permission from Ref. [50]. Copyright 2017 by Elsevier)

is small, the square superposition law has also been proven to be valid [58]. In the work of [38], it has been indicated that both these two superposition laws could offer a good fit of the yield stress when there exist three dominant defects, i.e. α'-phase particles, NiSiPCr-rich clusters and DLs, for neutron-irradiated Fe–Cr alloys. However, for ion-irradiated materials, the square superposition law is found to work better, especially when the plastic zone extends into the unirradiated region that the substrate softening effect becomes dominant, as illustrated in Fig. 4 [51].

2.2 Crystal plasticity based irradiation hardening model

In order to theoretically analyze the mechanical properties of irradiated materials, both the hardening mechanisms and evolution laws of irradiation-induced defects should be properly addressed. Within the framework of the classical crystal plasticity theory, deformation gradient $\mathbf{F}$ of materials can be decomposed into elastic and plastic parts, i.e.

$$\mathbf{F} = \mathbf{F}^{\mathrm{e}} \cdot \mathbf{F}^{\mathrm{p}}, \tag{10}$$

where the elastic and plastic parts are, respectively, denoted by the superscripts "e" and "p". The evolution rate of the plastic deformation gradient ($\dot{\mathbf{F}}^{\mathrm{p}}$) involving the contribution of sliding dislocations on different slip systems follows as

$$\dot{\mathbf{F}}^{\mathrm{p}} = \left(\sum_{\alpha=1}^{N_{\mathrm{s}}} \dot{\gamma}^{\alpha} \mathbf{s}^{\alpha} \otimes \mathbf{n}^{\alpha} \right) \cdot \mathbf{F}^{\mathrm{p}}, \tag{11}$$

where N_{s} is the number of slip systems. For FCC, BCC, and HCP metals, there are, respectively, 12, 48, and 12 slip systems that can be characterized by the Miller indices $\{111\}\langle 110\rangle$ (for FCC materials), $\{110\}\langle 111\rangle$, $\{112\}\langle 111\rangle$ and $\{123\}\langle 111\rangle$ (for BCC materials), as well as $\{0001\}\langle 1120\rangle$, $\{1100\}\langle 1120\rangle$ and $\{1011\}\langle 1123\rangle$ (for HCP materials). $\mathbf{n}^{\alpha}$ and $\mathbf{s}^{\alpha}$ are the unit vectors of the normal direction and slip direction of slip system α, respectively. $\dot{\gamma}^{\alpha}$ is the shearing slip rate on the α-th slip system, which depends on the resolved shear stress ($\tau^{\alpha}_{\mathrm{RSS}}$) and CRSS ($\tau^{\alpha}_{\mathrm{CRSS}}$), i.e.

$$\dot{\gamma}^{\alpha} = \dot{\gamma}^{\alpha} \left(\tau^{\alpha}_{\mathrm{RSS}}, \tau^{\alpha}_{\mathrm{CRSS}} \right). \tag{12}$$

With irradiation effect, $\tau^{\alpha}_{\mathrm{CRSS}}$ is determined by both the hardening contributions coming from irradiation defects and intrinsic material hardening mechanisms (e.g. the initial lattice resistance and network dislocation hardening). In recent years, a number of irradiation hardening models and their evolution laws have been extensively developed for FCC [59–64], BCC [36,65–70], and HCP materials [37,71,72], which can be categorized into two general groups, i.e. the scalar irradiation hardening model and tensorial irradiation hardening model as summarized in Table 1. For the latter, the dislocation-defect interaction and their evolution behavior are taken in a tensorial form, which tends to characterize the heterogeneous plastic deformation and spatial interaction between irradiation defects and dislocations as inspired by the simulation results of dislocations dynamics [73].

The first combination of the scalar irradiation hardening model with the crystal plasticity theory was performed in 2004 [59], in which an internal state variable was proposed to characterize the hardening contribution of SFTs in irradiated FCC copper. The general feature captured by this constitutive equation is that the yield stress increases with the density of irradiation defects. Concerning the mechanical behavior of irradiated zirconium alloys with HCP structures, the classical DBH model has been applied to characterize the effect of irradiation-induced DLs, which are inhomogeneously distributed in the prism, pyramidal and pyramidal slip systems [71]. Based on the parameterized model, the simulated stress–strain curves can match well with the experimental data under both transverse tensile test and internal pressure test. More recently, the irradiation effect on the yield stress and flow stress of single crystal iron is analyzed with the mechanism-based continuum dislocation dynamics [65], in which a modified DBH model is applied to express the irradiation resistance induced by the dislocation-DL interaction.

A tensorial damage descriptor variable is firstly proposed by Barton et al. [69] to describe the spatial interaction between dislocations and DLs that leads to the formation of localized plastic deformation. In their theoretical model, two critical tensors $\mathbf{H}$ and $\mathbf{N}$ are, respectively, defined for the irradiation defects and dislocations, i.e.

$$\mathbf{H} = (1/V) \sum 3 d_{\mathrm{def}} (\mathbf{I} - \mathbf{n} \otimes \mathbf{n}) \tag{13}$$

Table 1 Irradiation hardening and evolution models for different types of irradiated-induced defects

References	Hardening model of defects	Evolution model of defects	Defect type
[59]	$\tau_{\text{def}} = h_{\text{d}}\mu b\sqrt{N_{\text{def}}d_{\text{def}}}$	$\dot{N}_{\text{def}} = \frac{3}{2}N_{\text{def}}\dot{\varepsilon}^{\text{p}}$, $\dot{d}_{\text{SFT}} = -\frac{1}{2}d_{\text{def}}\dot{\varepsilon}^{\text{p}}$	SFTs in copper
[70]	$\tau_{\text{def}} = h_{\text{d}}\mu b\sqrt{N_{\text{def}}d_{\text{def}}}$	$\dot{N}_{\text{def}} = -\eta N_{\text{def}}\sum\lvert\dot{\gamma}\rvert$	DLs in zirconium alloys
[65]	$\tau_{\text{def}} = h_{\text{d}}\mu b(N_{\text{def}}d_{\text{def}})^{n}$	No	DLs in iron
[66–68,70]	$\tau_{\text{def}} = \mu b\sqrt{h_{\text{d}}N_{\text{def}}d_{\text{def}}}$	see Table 1 of Ref. [67]	DLs and voids in steel
[60]	$\tau_{\text{def}} = \chi\mu bh_{\text{d}}\sqrt{\sum LN_{\text{def}}d_{\text{def}}}$	$\dot{d}_{\text{def}} = \kappa_s(d_{\text{def}}^{\text{sat}} - d_{\text{def}})\dot{\gamma}$	SFTs in copper
[37]	$\tau_{\text{def}} = h_{\text{d}}\mu b\sqrt{N_{\text{def}}d_{\text{def}}}$	$\dot{\tau}_{\text{def}} = -f\tau_{\text{def}}$	DLs in zircaloy
[71]	$\tau_{\text{def}} = \chi\mu b\sqrt{LN_{\text{def}}d_{\text{def}}}$	$\dot{N}_{\text{def}} = -(\sum\rho_{\text{dis}})AN_{\text{def}}\frac{d_{\text{def}}}{b}\dot{\gamma}$	DLs in molybdenum
[61–64]	$\tau_{\text{def}} = \mu b\sqrt{h_{\text{d}}\sum\mathbf{N}:\mathbf{H}}$, $\mathbf{N} = \mathbf{n}\otimes\mathbf{n}$, $\mathbf{H} = N_{\text{def}}d_{\text{def}}(\mathbf{I}-\mathbf{n}\otimes\mathbf{n}+P_{\text{ann}}\delta\mathbf{n}\otimes\mathbf{n})$	$\dot{\mathbf{H}} = -\eta\sum(\mathbf{N}:\mathbf{H})\mathbf{N}\lvert\dot{\gamma}\rvert$	SFTs in copper
[36,69]	$\tau_{\text{def}} = \mu b\sqrt{h_{\text{d}}\mathbf{N}:\mathbf{H}}$, $\mathbf{N} = \mathbf{n}\otimes\mathbf{n}$, $\mathbf{H} = 1/V\sum 3d_{\text{def}}(\mathbf{I}-\mathbf{n}\otimes\mathbf{n})$	$\dot{\mathbf{H}} = -\eta\sum(\mathbf{N}:\mathbf{H})\mathbf{N}\lvert\dot{\gamma}\rvert$	DLs in iron and iron-copper alloys
[58]	$\tau_{\text{def}} = \mu b\sqrt{h_{\text{d}}\mathbf{N}:\mathbf{H}}$, $\mathbf{N} = \mathbf{n}\otimes\mathbf{n}$, $\mathbf{H} = 3N_{\text{def}}d_{\text{def}}(\mathbf{I}-\mathbf{n}\otimes\mathbf{n})$	$\dot{\mathbf{H}} = -\eta\sum(\mathbf{N}:\mathbf{H})(\mathbf{I}-\mathbf{n}\otimes\mathbf{n})\lvert\dot{\gamma}\rvert$	DLs in iron and Fe–Cr alloys

h_{d} is the defect hardening coefficient; μ is the shear modulus; b is the magnitude of Burgers vector; N_{def} is the number density of defects; d_{def} is the defect size; $\dot{\varepsilon}^{\text{p}}$ is the plastic strain rate; $\mathbf{n}$ is the normal direction of dislocation sliding plane; $\mathbf{I}$ is the second-order unit tensor; η is the defect annihilation parameter; n is a parameter obtained from dislocation dynamics; χ is a statistical parameter; $L = \omega_3 + (1-\omega_4)\delta^{\alpha\beta}$ is the defect interaction coefficient; κ_s is a parameter accounting the interaction of defects and gliding dislocations; P_{ann} is the defect annihilation probability; f is a linear softening parameter. SFTs and DLs denote, respectively, stacking fault tetrahedra and dislocation loops

and

$$\mathbf{N} = \mathbf{n}\otimes\mathbf{n}, \tag{14}$$

where V, d_{def}, $\mathbf{I}$ and $\mathbf{n}$ are, respectively, the simulation volume, average size of irradiation defects, second-order unit tensor and normal direction of the dislocation sliding plane. Combing the parameterized crystal plasticity theory with the finite element simulation method, the proposed model is able to capture the characteristic mechanical properties of neutron-irradiated ferritic alloys, including the plastic flow localization and strain softening [69]. Inspired by this work, Xiao et al. [61–64] expanded the theoretical framework to neutron-irradiated FCC metals with SFTs. Due to the three dimensional structure of SFTs, an interaction probability is involved in the hardening model when the sliding plane of dislocations is parallel to the habit plane of SFTs. Moreover, the effect of test temperature and interfaces are both incorporated in the developed constitutive equations to study the thermo-mechanical behaviors of irradiated materials with different intrinsic microstructures. It is indicated that the intrinsic interfaces, including the free surface of single crystals, grain boundary of nanocrystals, and twin boundary of nano-twinned polycrystals, play an important role in alleviating the degradation of the mechanical properties of irradiated materials.

The strain hardening behavior of irradiated materials is strongly dependent on the evolution of irradiation-induced defects and dislocations during the plastic deformation process. Up to now, several groups of evolution laws have been proposed for irradiation-induced DLs and SFTs [59–61,67], as summarized in Table 1. These evolution functions intrinsically account for the physical mechanisms as noticed in the numerical simulation results and experimental observations, i.e. irradiation defects are annihilated by the interaction with sliding dislocations, which results in the decrease of the defect density. Combining with the evolution laws for dislocations, which characterize the generation, annihilation and cross slip of sliding dislocations, the developed crystal plasticity theory can capture the dominant features of irradiation effects, including the decrease of the flow stress after the yield point, plastic flow localization and decrease of the strain hardening coefficient. When the initial density of irradiation defects is above a critical value, the decrease of the flow stress can be obviously noticed which originates from the dramatic decrease of the defect density. Due to the spatially dependent interaction between dislocations and irradiation defects, the annihilation of irradiation defects occurs on some specific slip systems, which renders the localized plastic deformation within the defect free channels. A typical tensorial evolution law that can effectively characterize the above mentioned deformation mechanisms has been proposed for irradiation-induced DLs [69] and SFTs [61], respectively, i.e.

$$\dot{\mathbf{H}} = -\eta \sum (\mathbf{N} : \mathbf{H})\mathbf{N}|\dot{\gamma}|, \tag{15}$$

where η is the annihilation coefficient for irradiation-induced defects. As indicated in Eq. (15) that the annihilation of irradiation defects happens when the plastic deformation is activated (i.e. $|\dot{\gamma}| > 0$), and the dislocation-defect interaction on all slip systems simultaneously contributes to the evolution of irradiation defects.

One should note that the above mentioned crystal plasticity theory with irradiation effect is only applicable for irradiated single crystals. In order to predict the mechanical properties of irradiated polycrystals based on the crystal plasticity theory, the application of an effective cross-scale method becomes vitally important. Nowadays, two general methods have been widely adopted, including the finite element method and self-consistent method. The former can be defined as the CPFEM when combining the crystal plasticity theory with the finite element method. The dominant advantage for the application of CPFEM is that it can simulate the macroscopic deformation behavior of irradiated samples under different loading conditions, e.g. axial tensile test and nano-indentation [60,66,70,74,75]. Meanwhile, the localized plastic deformation mechanisms can be effectively addressed, including the formation of defect free channels, void nucleation and micro-crack extension [66–68]. Whereas, it should be emphasized that the calculation with the CPFEM is quite time-consuming, especially for the irradiated polycrystals with numbers of individual grains, which makes it difficult to calibrate the parameters of the constitutive equations with various kinds of irradiation-induced defects.

As an alternative, the self-consistent method offers a promising approach to characterize the macroscopic stress–strain relationship of irradiated polycrystals, especially for the save of calculation time and convenient calibration of model parameters [76,77]. Recently, a theoretical framework, which combines the crystal plasticity based irradiation hardening model with the elastic–viscoplastic self-consistent (EVPSC) method, has been proposed for FCC polycrystals with irradiation effect [61–64]. At the grain level, the detailed dislocation network interaction, dislocation-defect interaction and evolution of these microstructures are involved in the irradiated crystal plasticity theory. With plastic deformation, the elastic and viscoplastic compliance tensor can be deduced from the constitutive equations, which act as the link to calculate the stress and strain rate of each individual grain with the assistant of the EVPSC method. A detailed flow chart for the application of the irradiated crystal plasticity theory with the EVPSC method is illustrated in Fig. 5. Corresponding programme codes of this theoretical model are offered in the electronic supplementary material with a brief user manual and some numerical examples.

In Fig. 6, the stress–strain relationships obtained from the CPFEM and EVPSC method are compared with corresponding experimental data for different nuclear structural materials under various irradiation conditions. It can be seen that: (1) the simulated results can match well with corresponding experimental data for irradiated FCC copper, BCC ion, Fe–Cr alloys and 9Cr-1Mo steels, as well as HCP Zirconium alloys and molybdenum; (2) the dominant features of the mechanical properties of irradiated materials could be characterized including the limited effect on the elastic deformation, increase of the yield stress, decrease of the strain hardening coefficient and occurrence of the plastic flow instability. Besides the analysis of the stress–strain relationship at macro-scale, the proposed model makes it possible to study the evolution of irradiation-induced defects on different slip systems and nucleation of micro-voids near the stress concentration sites at micro-scale [66,70], which can help understand the formation of localized plastic deformation and accelerated failure after irradiation.

In summary, the development of the theoretical models for the assessment of irradiation hardening has made significant progress in recent years, especially for the incorporation of the hardening model and evolution law of irradiation defects into the crystal plasticity theory. Whereas, these theoretical models are primarily developed under the conditions of moderate test temperatures and low irradiation doses, which makes it almost impossible to directly apply the proposed models to the even worse irradiation conditions, let alone the consideration of the accumulated defect clusters formed by the transmutation elements like helium and hydrogen bubbles. Moreover, the material failure criterion is not involved in the proposed theoretical framework, which make it only applicable before the flow stress reaches the ultimate material strength. Therefore, the following considerations should be addressed for the further development of the crystal plasticity theory framework with irradiation effect: (1) explore the deformation mechanisms at high irradiation doses and temperatures; (2) consider the synergistic effect of irradiation-induced defects and transmutation elements for the deformation behavior of neutron-irradiated materials at high irradiation doses; (3) incorporate the material failure criterion with irradiation effect into the crystal plasticity theory for the assessment of irradiation embrittlement under various irradiation conditions.

3 Theoretical model for irradiation embrittlement

A great challenge for the safety assessment of nuclear structural materials is the development of advanced embrittlement

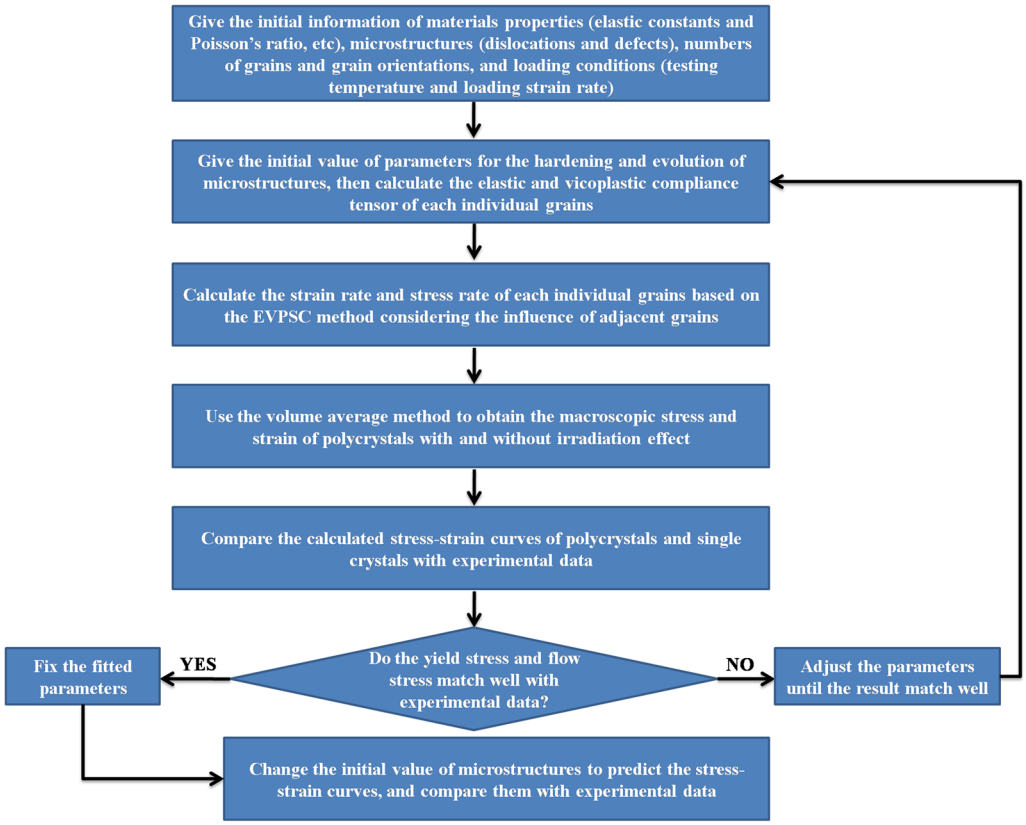

Fig. 5 Flow diagram for the application of the crystal plasticity theory with the EVPSC method to obtain the stress–strain relationship of polycrystals with irradiation effect

models [79–82]. Over the past decades, the development of the embrittlement model concerning the effect of irradiation-induced defects on the fracture toughness can be categorized into two stages. In the first stage, the linear-elastic fracture mechanics (LEFM) is applied when the failure of irradiated materials occurs with negligible plastic deformation. Under this condition, the fracture toughness is expressed by the parameter K_{IC} (i.e. the plane strain fracture toughness), which indicates the resistance of materials to the extension of unstable cracks [83]. There are two dominant shortcomings when applying the LEFM to assess the fracture toughness around the ductile brittle transition (DBT) region. (1) The tested samples should be large enough ensuring the valid measurement of the linear-elastic fracture toughness as requested by the K_{IC} test standard. (2) The data dispersion of the fracture toughness is obvious in the DBT region, therefore, a large number of specimens are required to characterize the material properties at a given test temperature. However, as mentioned in the previous section, the space within the nuclear reactors is quite limited, which dramatically restrict the application of the LEFM in the nuclear industry [84].

In the second stage, the development of the elasto-plastic fracture mechanics (EPFM) (since 1970s) allows the determination of the fracture toughness with much small specimens [84]. The EPFM is based on the J integral-resistance curve that is applied when the failure of irradiated materials happens accompanying the plastic deformation. Hereinto, the J integral characterizes the external work applied for the crack to propagate [83]. A typical application of this EPFM is the Master Curve approach [85,86] that has been widely used to analyze the irradiation effects on the fracture toughness-temperature relationship of irradiated materials (see Fig. 7) [87]. According to the ASTM Standard E1921-05, the fracture toughness as a function of the test temperature for a given failure probability is expressed as

$$K_{\mathrm{JC},P_{\mathrm{f}}} = 20 + \left[\ln\left(\frac{1}{1-P_{\mathrm{f}}}\right)\right]^{\frac{1}{4}} \cdot \left[11 + 77\mathrm{e}^{0.019(T-T_0)}\right], \tag{16}$$

where P_{f}, T and T_0 are, respectively, the failure probability, test temperature and reference temperature. Moreover, $K_{\mathrm{JC},P_{\mathrm{f}}}$ also represents the elastic-plastic equivalent stress intensity factor of an one-inch standardized test sample. If the thickness of tested samples is not one inch, the fracture toughness can be transformed through thefollowing equation

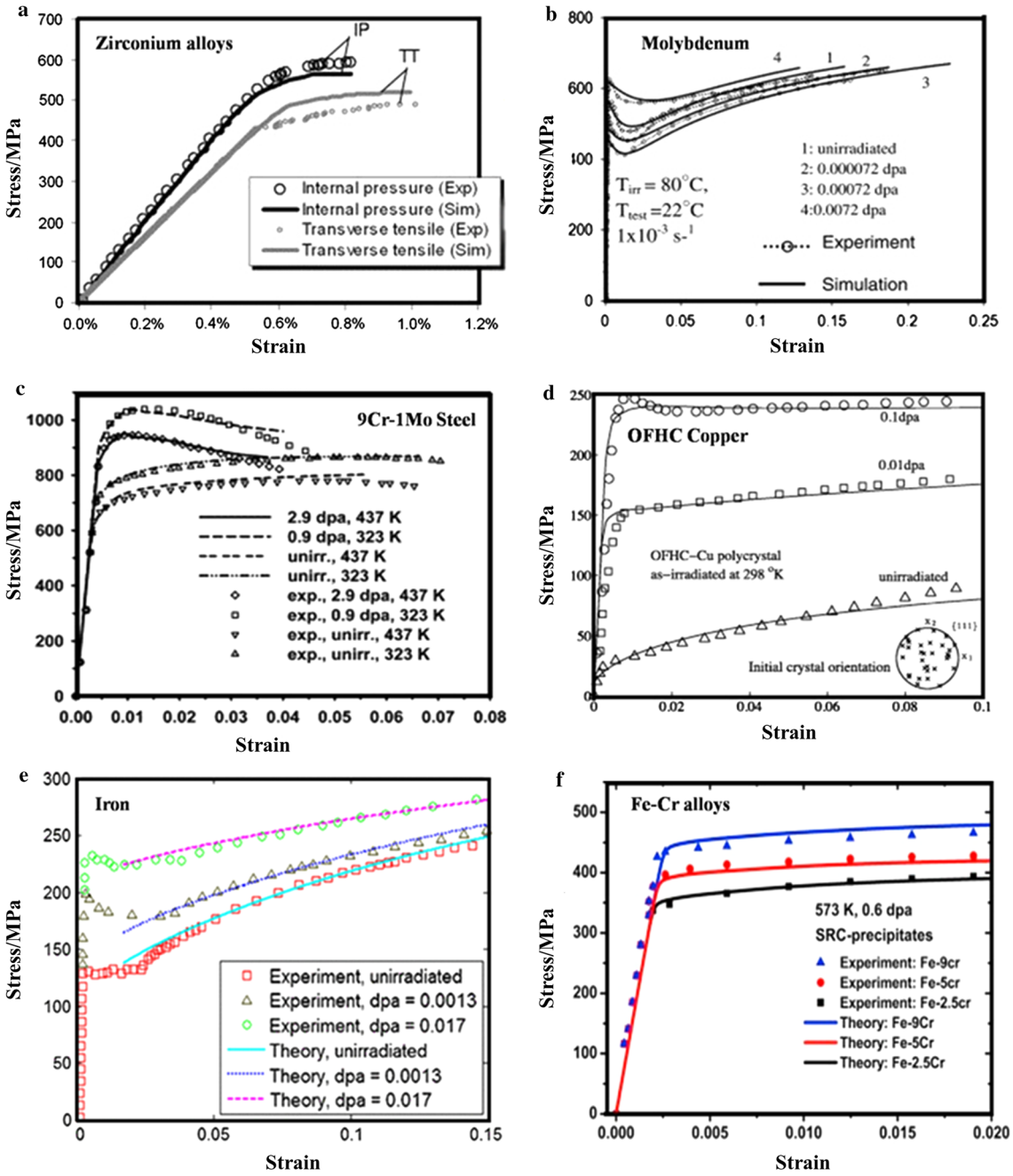

Fig. 6 Simulated stress–strain relationship (solid lines) of irradiated materials compared with corresponding experimental data (symbols). **a** Zirconium alloys tested at a strain rate of 1.6×10^{-4} s^{-1} and 623 K. (Reprinted with permission from Ref. [71]. Copyright 2008 by Elsevier). **b** Molybdenum tested at a strain rate of 1×10^{-3} s^{-1}. (Reprinted with permission from Ref. [72]. Copyright 2010 by Elsevier). **c** 9Cr-1Mo steels tested at a strain rate of 1×10^{-4} s^{-1}. (Reprinted with permission from Ref. [66]. Copyright 2012 by Elsevier). **d** OFHC Copper tested at a strain rate of 1.2×10^{-3} s^{-1} and 373 K. (Reprinted with permission from Ref. [60]. Copyright 2014 by Elsevier). **e** Iron tested at a strain rate of 6×10^{-5} s^{-1} and 293 K. (Reprinted with permission from Ref. [78]. Copyright 2015 by Springer). **f** Fe–Cr alloys tested at a strain rate of 2.8×10^{-4} s^{-1}. (Reprinted with permission from Ref. [57]. Copyright 2016 by Elsevier)

$$K_{B_1} = K_{\min} + (K_{B_2} - K_{\min}) \left(\frac{B_2}{B_1} \right)^{\frac{1}{4}}, \tag{17}$$

where $K_{\min}$ is the lower limit value of the fracture toughness. B_1 and B_2 are the thicknesses of test samples. With the application of Eq. (16), the confidence bounds of the distribution could be obtained, e.g. $P_f = 0.01$ or $P_f = 0.05$ for the lower bound and $P_f = 0.95$ or $P_f = 0.99$ for the upper bound. With $P_f = 0.5$, the relationship between the fracture toughness and test temperature is referred to the Master Curve,

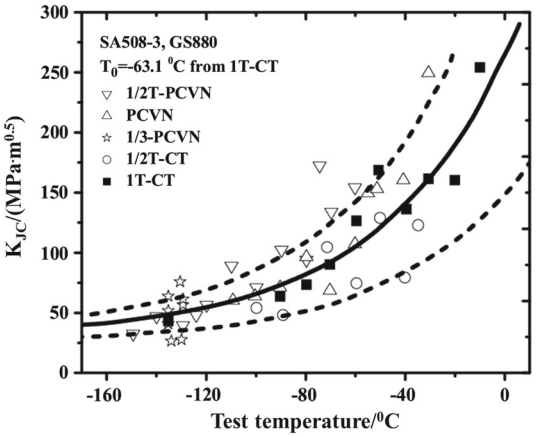

Fig. 7 Measured results obtained from the Master curve fracture toughness test for different types of SA508-3 PRV steel . (Reprinted with permission from Ref. [87]. Copyright 2008 by Elsevier)

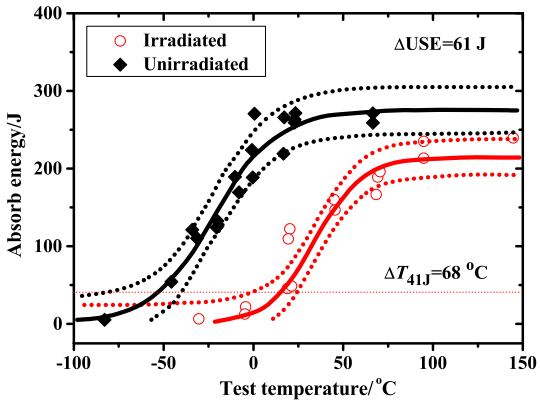

Fig. 8 Relationship of Charpy impact absorb energy and test temperature for irradiated and unirradiated A508-3 steels . (Reprinted with permission from Ref. [90]. Copyright 2017 by Elsevier)

i.e.

$$K_{\mathrm{JC},P_f=0.5} = 30 + 70\mathrm{e}^{0.019(T-T_0)}, \tag{18}$$

where T_0 is defined when $K_{\mathrm{JC},P_f=0.5} = 100\ \mathrm{MPa}\cdot\mathrm{m}^{1/2}$. The advantage for the application of the Master Curve method is that it is convenient to calculate K_{JC} based on the value of the J integral, which dramatically avoids the requirement of numbers of testing samples. Moreover, the application of the probability statistics is able to effectively address the divergence of experimental data. Whereas, the existing problem is how to accurately calculate the value of T_0 considering the limited experimental data, which is very important for the prediction of the fracture toughness at different test temperatures based on Eq. (16).

Besides the theoretical analysis of the fracture toughness with irradiation effect, attention has also been paid to the theoretical model for the ductile brittle transition temperature (DBTT) [36,88], which is determined by the relationship between the Charpy impact energy and test temperature. Through the application of the Burr distribution function, the Charpy impact energy as a function of the test temperature is found to follow a sigmoidal curve [89]. With irradiation effect, the sigmoidal curve tends to shift to the low temperature region as has been indicated by numbers of experimental data (see Fig. 8 for instance). Therefore, it is believed that the analysis of the irradiation effect on the parameters characterizing the Burr distribution function is an effective method to theoretically address the influences of irradiation dose and temperature on the DBTT shift [89].

As one can tell, the above mentioned theoretical models mainly concern the influence of irradiation defects on the fracture behavior of irradiated materials around the DBT region. From another point of view, some progress has also been made to develop the theoretical models in the ductile region [67,91]. For instance, in order to analyze the plastic deformation and fracture properties of reactor pressure vessel steels, Murakami et al. [92] developed a model that the constitutive equations are within the framework of the irreversible thermodynamics theory. The influence of irradiation-induced defects is taken into account for the evolution of the yield stress and work hardening, as well as the mechanism of void nucleation due to the pile-up of dislocations. By comparing with the experimental data of irradiated steels, the numerical results could not only characterize the increase of the yield stress and tensile strength, but also the reduction of the fracture strain. Moreover, the constitutive equations could help analyze the fracture toughness of structural components when incorporated into the FEM simulation, and predict the DBTT shift once the temperature effect is involved.

Another mechanism-based model has been developed by Margolin et al. [93,94], which can predict the fracture strain and fracture toughness of austenitic steels under neutron irradiation. In this model, a failure criterion is established to account for the nucleation, growth and coalescence of voids under continuous deformation. Based on the analysis of this theoretical model, the irradiation embrittlement of austenitic steels is attributed to the formation of channel fracture or intergranular fracture, which, respectively, originates from the shearing of voids under the channel deformation or twinning when irradiation-induced defects weaken the strength of grain boundaries [93,94].

To sum up, the theoretical models for the irradiation embrittlement have been developed for decades within the framework of fracture mechanics, and applied in nuclear industries to assess the shift of the DBTT and evolution of the fracture toughness as a function of the test temperature. It should be noted that most of these models are phenomenological hence are limited with experimental data, and can hardly be applied to predict the failure of other nuclear structural materials when changing the irradiation condi-

tions. To solve this tough problem, theoretical models based on physical mechanisms should be developed to take into account the evolution of microstructures [95] and temperature effect [96,97]. The theoretical study of the irradiation embrittlement is difficult as a number of intrinsic materials properties and extrinsic environmental conditions affect the failure mode of irradiated materials. Therefore, the development of a unified theoretical model for the analysis of the irradiation embrittlement from micro-scale to macro-scale still deserves further efforts.

4 Summary and outlook

This review provides a systematic summary of the research progress of the irradiation hardening and embrittlement from the aspects of theoretical modelling. The relation between irradiation-induced defects and mechanical properties of nuclear materials has been addressed over the last decades [1,20,40]. According to the previous discussions, one can see that a number of research works have been performed to understand the fundamental mechanisms related to the irradiation hardening and embrittlement. However, the current knowledge on these mechanisms is far from being complete, and further aspects need to be investigated.

Firstly, it is meaningful to extend the study of the irradiation hardening and embrittlement to the conditions of high irradiation temperature and dose, which are close to the expected service environment of nuclear materials in the future fission and fusion reactors. Based on the existing knowledge of the irradiation effect at moderate irradiation conditions, the mechanical properties of nuclear materials under even worse irradiation conditions can hardly be predicted as the fundamental deformation mechanisms can be quite different. Therefore, the combined research including experiments, simulations and theories is necessary for the comprehension of the irradiation effects at high irradiation dose and temperature.

Secondly, the interchangeability study of neutron irradiation and ion irradiation should be emphasized as the performance of neutron irradiation experiments is much more complicated than that of ion irradiation experiments, which makes ion irradiation be a promising alternative to study the irradiation effect. This study should include the comparison of both irradiation-induced microstructures and mechanical properties. Due to the difference in the impact energy, electrical property, particle mass and irradiation rate of neutrons and ions, the density and distribution of irradiation-induced defects are not the same at a fixed irradiation dose and temperature. Moreover, conventional mechanical testing methods adopted for neutron-irradiated samples are not applicable for ion-irradiated materials, mainly due to the limited irradiated layer and non-uniform damage distribution. Consequently, one should be cautious when directly comparing the mechanical properties of neutron- and ion-irradiated materials.

Thirdly, attention should be paid to the establishment of a complete theory framework for the explanation, analysis and prediction of the embrittlement behavior induced by irradiation-induced defects. Comparing with the unambiguous understanding of the irradiation hardening, the fundamental mechanisms for the comprehension of the irradiation embrittlement are still not very clear. It is expected that related theoretical models, based on the physical understanding of the evolution of microstructures within and between adjacent grains, can be developed to help investigate the reduction of ductility, decrease of fracture toughness and increase of DBTT after irradiation.

Finally, the establishment of an effective multi-scale simulation framework to assess the irradiation effects is increasingly important for the analysis of the mechanical properties of the newly developed irradiation-resistant materials. However, it is still a big challenge as the study of irradiation effects covers the spatial scale from nanometers to meters, and the temporal scale from picoseconds to years. One possible solution method is to set up an effective data transmission strategy for the simulation methods at different scales, and validate the rationality and accuracy of the method by comparing the predicted numerical results with corresponding experimental data. Once this multi-scale modelling method works, it can, for sure, facilitate the R&D of nuclear structural materials.

It is envisioned that this review could help understand the basic features of the irradiation hardening and embrittlement at moderate irradiation conditions, provide scientific insights to the fundamental mechanisms resulting in the degradation of the mechanical properties of irradiated materials, and help the R&D of next-generation nuclear materials that could tolerate the neutron damage levels expected in the future fission and fusion reactors.

Acknowledgements This work was supported by the National Natural Science foundation of China (NSFC) (Grants 11632001, 11521202, 11802344) and Natural Science Foundation of Hunan Province, China (Grant 2019JJ50809). Xiao thanks the initial funding supported by Central South University.

References

1. Zinkle, S.J., Snead, L.L.: Designing radiation resistance in materials for fusion energy. In: Clarke, D.R. (ed.) Annual Review of Materials Research, pp. 241–267. Annual Reviews, Palo Alto (2014)
2. Shimada, M., Campbell, D.J., Mukhovatov, V., et al.: Progress in the ITER physics basis. Chapter 1: overview and summary. Nucl. Fusion **47**, S1–S17 (2007)
3. Zinkle, S.J.: Fusion materials science: overview of challenges and recent progress. Phys. Plasmas **12**, 058101 (2005)

4. Li, M., Eldrup, M., Byun, T.S., et al.: Low temperature neutron irradiation effects on microstructure and tensile properties of molybdenum. J. Nucl. Mater. **376**, 11–28 (2008)
5. Garner, F.A., Toloczko, M.B., Sencer, B.H.: Comparison of swelling and irradiation creep behavior of fcc-austenitic and bcc-ferritic/martensitic alloys at high neutron exposure. J. Nucl. Mater. **276**, 123–142 (2000)
6. Garner, F.A., Toloczko, M.B.: Irradiation creep and void swelling of austenitic stainless steels at low displacement rates in light water energy systems. J. Nucl. Mater. **251**, 252–261 (1997)
7. Yamashita, S., Yano, Y., Tachi, Y., et al.: Effect of high dose/high temperature irradiation on the microstructure of heat resistant 11Cr ferritic/martensitic steels. J. Nucl. Mater. **386**, 135–139 (2009)
8. Terentyev, D.A., Malerba, L., Chakarova, et al.: Displacement cascades in FE-CR: a molecular dynamics study. J. Nucl. Mater. **349**, 119–132 (2006)
9. Terentyev, D.A., Malerba, L., Hou, M.: Dimensionality of interstitial cluster motion in bcc-Fe. Phys. Rev. B **75**, 104108 (2007)
10. Nordlun, K., Zinkle, S.J., Sand, A.E., et al.: Primary radiation damage: a review of current understanding and models. J. Nucl. Mater. **512**, 450–479 (2018)
11. Terentyev, D., Bacon, D.J., Osetsky, Y.N.: Interaction of an edge dislocation with voids in alpha-iron modelled with different interatomic potentials. J. Phys. Condens. Mat. **20**, 445007 (2008)
12. Becquart, C.S., Domain, C.: Modeling microstructure and irradiation effects. Metall. Mater. Tans. A **42A**, 852–870 (2011)
13. Singh, B.N., Leffers, T., Horsewell, A.: Dislocation and void segregation in copper during neutron irradiation. Pholos. Mag. **53**, 233–242 (1986)
14. Brimbal, D., Decamps, B., Barbu, A., et al.: Dual-beam irradiation of alpha-iron: heterogeneous bubble formation on dislocation loops. J. Nucl. Mater. **418**, 313–315 (2011)
15. Kuksenko, V., Pareige, C., Pareige, P.: Cr precipitation in neutron irradiated industrial purity Fe–Cr model alloys. J. Nucl. Mater. **432**, 160–165 (2013)
16. Briceno, M., Kacher, J., Robertson, I.M.: Dynamics of dislocation interactions with stacking-fault tetrahedra at high temperature. J. Nucl. Mater. **433**, 390–396 (2013)
17. Yang, S., Yang, Z., Wang, H., et al.: Effect of laser and/or electron beam irradiation on void swelling in SUS316L austenitic stainless steel. J. Nucl. Mater. **488**, 215–221 (2017)
18. Was, G.S., Bruemmer, S.M.: Effects of irraidation on intergranular stress corrosion cracking. J. Nucl. Mater. **216**, 326–347 (1994)
19. Chopra, O.K., Rao, A.S.: A review of irradiation effects on LWR core internal materials—IASCC susceptibility and crack growth rates of austenitic stainless steels. J. Nucl. Mater. **409**, 235–256 (2011)
20. Knaster, J., Moeslang, A., Muroga, T.: Materials research for fusion. Nat. Phys. **12**, 424–434 (2016)
21. Acosta, B., Sevini, F.: Evaluation of irradiation damage effect by applying electric properties based techniques. Nucl. Eng. Des. **229**, 165–173 (2004)
22. Song, C.: Irradiation effects on Zr-2.5Nb in power reactors. CNL Nucl. Rev. **5**, 17–36 (2016)
23. Azevedo, C.R.F.: A review on neutron-irradiation-induced hardening of metallic components. Eng. Fail. Anal. **18**, 1921–1942 (2011)
24. Byun, T.S., Farrell, K., Li, M.: Deformation in metals after low-temperature irradiation: part I—mapping macroscopic deformation modes on true stress-dose plane. Acta Mater. **56**, 1044–1055 (2008)
25. Byun, T.S., Farrell, K., Li, M.: Deformation in metals after low-temperature irradiation: part II—irradiation hardening, strain hardening, and stress ratios. Acta Mater. **56**, 1056–1064 (2008)
26. Kuksenko, V., Pareige, C., Genevois, C., et al.: Effect of neutron-irradiation on the microstructure of a Fe-12at.%Cr alloy. J. Nucl. Mater. **415**, 61–66 (2011)
27. Pokor, C., Brechet, Y., Dubuisson, P., et al.: Irradiation damage in 304 and 316 stainless steels: experimental investigation and modeling. Part I: evolution of the microstructure. J. Nucl. Mater. **326**, 19–29 (2004)
28. Yan, C., Wang, R., Wang, Y., et al.: Effects of ion irradiation on microstructure and properties of zirconium alloys—a review. Nucl. Eng. Technol. **47**, 323–331 (2015)
29. Chen, Y.: Irradiation effects of ht-9 martensitic steel. Nucl. Eng. Technol. **45**, 311–322 (2013)
30. Scott, P.: A review of irradiation assisted stress corrosion cracking. J. Nucl. Mater. **211**, 101–122 (1994)
31. Xu, S., Zheng, W., Yang, L.: A review of irradiation effects on mechnical properties of candidate SCWR fuel cladding alloys for design considerations. CNL Nucl. Rev. **5**, 309–331 (2016)
32. Kurtz, R.J., Alamo, A., Lucon, E., et al.: Recent progress toward development of reduced activation ferritic/martensitic steels for fusion structural applications. J. Nucl. Mater. **386–88**, 411–417 (2009)
33. Shin, C., Jin, H.-H., Kim, M.-W.: Evaluation of the depth-dependent yield strength of a nanoindented ion-irradiated Fe–Cr model alloy by using a finite element modeling. J. Nucl. Mater. **392**, 476–481 (2009)
34. Yu, L., Xiao, X., Chen, L., et al.: A micromechanical model for nano-metallic-multilayers with helium irradiation. Int. J. Solids Struct. **102**, 267–274 (2016)
35. Dunn, A., Dingreville, R., Capolungo, L.: Multi-scale simulation of radiation damage accumulation and subsequent hardening in neutron-irradiated alpha-Fe. Modell. Simul. Mater. Sci. Eng. **24**, 015005 (2016)
36. Chakraborty, P., Biner, S.B.: Crystal plasticity modeling of irradiation effects on flow stress in pure-iron and iron–copper alloys. Mech. Mater. **101**, 71–80 (2016)
37. Erinosho, T.O., Dunne, F.P.E.: Strain localization and failure in irradiated zircaloy with crystal plasticity. Int. J. Plast. **71**, 170–194 (2015)
38. Bergner, F., Pareige, C., Hernandez-Mayoral, M., et al.: Application of a three-feature dispersed-barrier hardening model to neutronirradiated Fe–Cr model alloys. J. Nucl. Mater. **448**, 96–102 (2014)
39. Orowan, E.: A type of plastic deformation new in metals. Nature **149**, 643–644 (1942)
40. Singh, B.N., Foreman, A.J.E., Trinkaus, H.: Radiation hardening revisited: role of intracascade clustering. J. Nucl. Mater. **249**, 103–115 (1997)
41. Friedel, J.: On the linear work hardening mate of face-centered cubic single crystals. Philos. Mag. **46**, 1169–1186 (1955)
42. Kroupa, F., Hirsch, P.B.: Elastic interaction between prismatic dislocation loops and straight dislocations. Discuss. Faraday Soc. **38**, 49–55 (1964)
43. Bacon, D.J., Kocks, U.F., Scattergood, R.O.: The effect of dislocation self-interaction on the Orowan stress. Philos. Mag. **28**, 1241–1263 (1973)
44. Kasada, R., Takayama, Y., Yabuuchi, K., et al.: A new approach to evaluate irradiation hardening of ion-irradiated ferritic alloys by nano-indentation techniques. Fusion Eng. Des. **86**, 2658–2661 (2011)
45. Liu, P.P., Wan, F.R., Zhan, Q.: A model to evaluate the nano-indentation hardness of ion-irradiated materials. Nucl. Instrum. Methods B **342**, 13–18 (2015)
46. Oka, H., Sato, Y., Hashimoto, N., et al.: Evaluation of multi-layered hardness in ion-irradiated stainless steel by nano-indentation technique. J. Nucl. Mater. **462**, 470–474 (2015)
47. Takayama, Y., Kasada, R., Yabuuchi, K., et al.: Evaluation of irradiation hardening of Fe-ion irradiated F82H by nano-indentation techniques. In: Nie, J.F. and Morton, A. (eds.) Pricm 7, pts 1–3. p. 2915 (2010)

48. Yabuuchi, K., Kuribayashi, Y., Nogami, S., et al.: Evaluation of irradiation hardening of proton irradiated stainless steels by nanoindentation. J. Nucl. Mater. **446**, 142–147 (2014)
49. Xiao, X., Yu, L.: A hardening model for the cross-sectional nanoindentation of ion-irradiated materials. J. Nucl. Mater. **511**, 220–230 (2018)
50. Xiao, X., Chen, Q., Yang, H., et al.: A mechanistic model for depth-dependent hardness of ion irradiated metals. J. Nucl. Mater. **485**, 80–89 (2017)
51. Xiao, X., Yu, L.: Comparison of linear and square superposition hardening models for the surface nanoindentation of ion-irradiated materials. J. Nucl. Mater. **503**, 110–115 (2018)
52. Misra, A., Hirth, J.P., Hoagland, R.G.: Length-scale-dependent deformation mechanisms in incoherent metallic multilayered composites. Acta Mater. **53**, 4817–4824 (2005)
53. Huang, H.F., Li, D.H., Li, J.J., et al.: Nanostructure variations and their effects on mechanical strength of Ni-17Mo-7Cr alloy under Xenon ion irradiation. Mater. Trans. **55**, 1243–1247 (2014)
54. Liu, X., Wang, R., Jiang, J., et al.: Slow positron beam and nanoindentation study of irradiation-related defects in reactor vessel steels. J. Nucl. Mater. **451**, 249–254 (2014)
55. Liu, X., Wang, R., Ren, A., et al.: Evaluation of radiation hardening in ion-irradiated Fe based alloys by nanoindentation. J. Nucl. Mater. **444**, 1–6 (2014)
56. Li, S., Wang, Y., Dai, X., et al.: Evaluation of hardening behaviors in ion-irradiated Fe-9Cr and Fe-20Cr alloys by nanoindentation technique. J. Nucl. Mater. **478**, 50–55 (2016)
57. Xiao, X., Terentyev, D., Yu, L., Bakaev, A., et al.: Investigation of the thermo-mechanical behavior of neutron-irradiated Fe–Cr alloys by self consistent plasticity theory. J. Nucl. Mater. **477**, 123–133 (2016)
58. Hiratani, M., Bulatov, V.V.: Solid-solution hardening by point-like obstacles of different kinds. Philos. Mag. Lett. **84**, 461–470 (2004)
59. Arsenlis, A., Wirth, B.D., Rhee, M.: Dislocation density-based constitutive model for the mechanical behaviour of irradiated Cu. Philos. Mag. **84**, 3617–3635 (2004)
60. De Rahul, S.: Multiscale modeling of irradiated polycrystalline fcc metals. Int. J. Solids Struct. **51**, 3919–3930 (2014)
61. Xiao, X., Song, D., Chu, H., et al.: Mechanical behaviors of irradiated fcc polycrystals with nanotwins. Int. J. Plast. **74**, 110–126 (2015)
62. Xiao, X.Z., Song, D.K., Xue, J.M., et al.: A size-dependent tensorial plasticity model for fcc single crystal with irradiation. Int. J. Plast. **65**, 152–167 (2015)
63. Xiao, X.Z., Song, D.K., Chu, H.J., et al.: Mechanical properties for irradiated face-centred cubic nanocrystalline metals. Proc. R. Soc. A Math. Phy. **471**, 20140832 (2015)
64. Xiao, X., Song, D., Xue, J., et al.: A self-consistent plasticity theory for modeling the thermo-mechanical properties of irradiated fcc metallic polycrystals. J. Mech. Phys. Solids **78**, 1–16 (2015)
65. Li, D., Zbib, H., Sun, X., et al.: Predicting plastic flow and irradiation hardening of iron single crystal with mechanism-based continuum dislocation dynamics. Int. J. Plast. **52**, 3–17 (2014)
66. Patra, A., McDowell, D.L.: Continuum modeling of localized deformation in irradiated bcc materials. J. Nucl. Mater. **432**, 414–427 (2013)
67. Patra, A., McDowell, D.L.: A void nucleation and growth based damage framework to model failure initiation ahead of a sharp notch in irradiated bcc materials. J. Mech. Phys. Solids **74**, 111–135 (2015)
68. Patra, A., McDowell, D.L.: Crystal plasticity investigation of the microstructural factors influencing dislocation channeling in a model irradiated bcc material. Acta Mater. **110**, 364–376 (2016)
69. Barton, N.R., Arsenlis, A., Marian, J.: A polycrystal plasticity model of strain localization in irradiated iron. J. Mech. Phys. Solids **61**, 341–351 (2013)
70. Patra, A., McDowell, D.L.: Crystal plasticity-based constitutive modelling of irradiated bcc structures. Philos. Mag. **92**, 861–887 (2012)
71. Onimus, F., Bechade, J.-L.: A polycrystalline modeling of the mechanical behavior of neutron irradiated zirconium alloys. J. Nucl. Mater. **384**, 163–174 (2009)
72. Krishna, S., De, S.: A temperature and rate-dependent micromechanical model of molybdenum under neutron irradiation. Mech. Mater. **43**, 99–110 (2011)
73. Arsenlis, A., Rhee, M., Hommes, G., et al.: A dislocation dynamics study of the transition from homogeneous to heterogeneous deformation in irradiated body-centered cubic iron. Acta Mater. **60**, 3748–3757 (2012)
74. Saleh, M., Zaidi, Z., Ionescu, M., et al.: Relationship between damage and hardness profiles in ion irradiated ss316 using nanoindentation-experiments and modelling. Int. J. Plast. **86**, 151–169 (2016)
75. Saleh, M., Xu, A., Hurt, C., et al.: Oblique cross-section nanoindentation for determining the hardness change in ion-irradiated steel. Int. J. Plast. **112**, 242–256 (2019)
76. Deo, C., Tom, C., Lebensohn, R., et al.: Modeling and simulation of irradiation hardening in structural ferritic steels for advanced nuclear reactors. J. Nucl. Mater. **377**, 136–140 (2008)
77. Li, D., Zbib, H., Garmestani, H., et al.: Modeling of irradiation hardening of polycrystalline materials. Comp. Mater. Sci. **50**, 2496–2501 (2011)
78. Song, D., Xiao, X., Xue, J., et al.: Mechanical properties of irradiated multi-phase polycrystalline bcc materials. Acta Mech. Sin. **31**, 191–204 (2015)
79. Odette, G.R., Nanstad, R.K.: Predictive reactor pressure vessel steel irradiation embrittlement models: issues and opportunities. JOM **61**, 17–23 (2009)
80. Chen, Z.-A., Wang, L.Y., Chao, Y.-J., et al.: A constraintequivalent approach for assessing fracture toughness of RPV steels under neutron irradiation. Nucl. Eng. Des. **250**, 53–59 (2012)
81. Minkin, A.I., Margolin, B.Z., Smirnov, V.I., et al.: Improvement of a model to predict static fracture toughness of austenitic materials under neutron irradiation. Inorg. Mater. Appl. Res. **5**, 617–25 (2014)
82. Lu, Z., Faulkner, R.G., Flewitt, P.E.J.: Irradiation-induced impurity segregation and ductile-to-brittle transition temperature shift in high chromium ferritic/martensitic steels. J. Nucl. Mater. **367**, 621–626 (2007)
83. Chopra, O.K., Rao, A.S.: A review of irradiation effects on LWR core internal materials-neutron embrittlement. J. Nucl. Mater. **412**, 195–208 (2011)
84. Scibetta, M., Ferreno, D., Gorrochategui, I., et al.: Characterisation of the fracture properties in the ductile to brittle transition region of the weld material of a reactor pressure vessel. J. Nucl. Mater. **411**, 25–40 (2011)
85. Wallin, K., Saario, T., Torronen, K.: Statistical model for carbide induced brittle fracture in steel. Metal Sci. **18**, 13–16 (1984)
86. Wallin, K.: The scatter in KIC results. Eng. Fract. Mech. **19**, 1085–1093 (1984)
87. Lee, B.-S., Kim, M.-C., Kim, M.-W., et al.: Master curve techniques to evaluate an irradiation embrittlement of nuclear reactor pressure vessels for a long-term operation. Int. J. Press. Vessels Pip. **85**, 593–599 (2008)
88. Kotrechko, S., Meshkov, Y.: A new approach to estimate irradiation embrittlement of pressure vessel steels. Int. J. Press. Vessels Pip. **85**, 336–343 (2008)
89. Moskovic, R., Jordinson, C., Stephens, D.A., et al.: A bayesian analysis of the influence of neutron irradiation on embrittlement in ferritic submerged arc weld metal. Metall. Mater. Trans. A **31**, 445–459 (2000)

90. Lin, Y., Yang, W., Tong, Z.F., et al.: Charpy impact test on A508-3 steel after neutron irradiation. Eng. Fail. Anal. A **82**, 733–740 (2017)
91. Konstantinovic, M.J.: Probabilistic fracture mechanics of irradiation assisted stress corrosion cracking in stainless steels. In: 21st European conference on fracture, vol. 2, pp. 3792–3798 (2016)
92. Murakami, S., Miyazaki, A., Mizuno, M.: Modeling of irradiation embrittlement of reactor pressure vessel steels. J. Eng. Matter. Technol. ASME **122**, 60–66 (2000)
93. Margolin, B., Sorokin, A., Smirnov, V., et al.: Physical and mechanical modelling of neutron irradiation effect on ductile fracture. Part 1. Prediction of fracture strain and fracture toughness of austenitic steels. J. Nucl. Mater. **452**, 595–606 (2014)
94. Margolin, B., Sorokin, A.: Physical and mechanical modeling of the neutron irradiation effect on ductile fracture. Part 2. Prediction of swelling effect on drastic decrease in strength. J. Nucl. Mater. **452**, 607–613 (2014)
95. Kayano, H., Kimura, A., Narui, M., et al.: Irradiation embrittlement of neutron-irradiation low activation ferritic steels. J. Nucl. Mater. **155**, 978–981 (1988)
96. Harries, D.R.: Neutron irradiation-induced embrittlement in type 316 and other austenitic steels and alloys. J. Nucl. Mater. **82**, 2–21 (1979)
97. Porter, D.L., Garner, F.A.: Irradiation creep and embrittlement behavior of AISI 316 stainless steel at very high neutron fluences. J. Nucl. Mater. **159**, 114–121 (1988)